

# Longitudinal Analysis of Structural and Functional Changes in Presence of Reticular Pseudodrusen Associated With Age-Related Macular Degeneration

Marlene Sassmannshausen,<sup>1,2</sup> Maximilian Pfau,<sup>1-3</sup> Sarah Thiele,<sup>1,2</sup> Rolf Fimmers,<sup>4</sup> Julia S. Steinberg,<sup>1</sup> Monika Fleckenstein,<sup>1,5</sup> Frank G. Holz,<sup>1,2</sup> and Steffen Schmitz-Valckenberg<sup>1,2,5</sup>

<sup>1</sup>Department of Ophthalmology, University of Bonn, Bonn, Germany

<sup>2</sup>GRADE Reading Center, Bonn, Germany

<sup>3</sup>Department of Biomedical Data Science, Stanford University, Stanford, California, United States

<sup>4</sup>Institute for Medical Biometry, Informatics and Epidemiology, University of Bonn, Medical Faculty, Bonn, Germany

<sup>5</sup>John A. Moran Eye Center, University of Utah, Salt Lake City, Utah, United States

Correspondence: Steffen Schmitz-Valckenberg, MD, FEBO, Department of Ophthalmology, University of Bonn, Ernst-Abbe-Str. 2, 53127 Bonn, Germany; [steffen.schmitz-valckenberg@ukb.uni-bonn.de](mailto:steffen.schmitz-valckenberg@ukb.uni-bonn.de).

Received: December 24, 2019

Accepted: July 9, 2020

Published: August 11, 2020

Citation: Sassmannshausen M, Pfau M, Thiele S, et al. Longitudinal analysis of structural and functional changes in presence of reticular pseudodrusen associated with age-related macular degeneration. *Invest Ophthalmol Vis Sci.* 2020;61(10):19. <https://doi.org/10.1167/iovs.61.10.19>

**PURPOSE.** To examine longitudinal changes of retinal thickness and retinal sensitivity in patients with intermediate age-related macular degeneration (iAMD) and predominantly reticular pseudodrusen (RPD).

**METHODS.** At baseline 30 eyes of 25 iAMD patients underwent optical coherence tomography imaging, mesopic and scotopic fundus-controlled perimetry (FCP) with follow-up examinations at month 12 (20 eyes), 24 (12 eyes), and 36 (11 eyes). Thicknesses of different retinal layers and results of FCP testing (n = 56 stimuli) were spatially and longitudinally analyzed using linear mixed-effects models.

**RESULTS.** At baseline, the thickness of the partial outer retinal layer (pORL, 70.21 vs. 77.47  $\mu\text{m}$ ) and both mesopic (16.60 vs. 18.72 dB) and scotopic (12.14 vs. 18.67 dB) retinal sensitivity were decreased in areas with RPD compared with unremarkable areas ( $P < 0.001$ ). Over three years, mean change of pORL was  $-0.66$  normative standard deviation (SD; i.e., z-score,  $P < 0.001$ ) for regions with existing RPD,  $-0.40$  SD ( $P < 0.001$ ) for regions with new occurring RPD, and  $-0.17$  SD ( $P = 0.041$ ) in unremarkable regions. Decrease of scotopic and mesopic sensitivity over three years was more pronounced in areas with existing ( $-3.51$  and  $-7.76$  dB) and new occurring RPD ( $-2.06$  and  $-5.97$  dB). Structure-function analysis revealed that 1 SD decrease of pORL thickness was associated with a sensitivity reduction of 3.47 dB in scotopic and 0.79 dB in mesopic testing.

**CONCLUSIONS.** This study demonstrates progressive outer retinal degeneration and impairment of photoreceptor function in eyes with iAMD and RPD over three years. Preservation of outer retinal thickness and reduction of RPD formation may constitute meaningful surrogate endpoints in interventional trials on eyes with AMD and RPD aiming to slow outer retinal degeneration.

**Keywords:** fundus-controlled perimetry, microperimetry, scotopic, mesopic, MP-1S, age-related macular degeneration, SD-OCT, retinal imaging, reticular pseudodrusen, RPD, subretinal drusenoid deposits, SDD

Age-related macular degeneration (AMD) is the leading cause of visual impairment in older individuals in industrialized countries.<sup>1</sup> Although the early and intermediate stage of disease is typically hallmarked by soft drusen,<sup>2</sup> a subset of patients presents with predominantly reticular pseudodrusen (RPD).<sup>3,4</sup> These RPD, also termed as reticular drusen or subretinal drusenoid deposits (SDD), have histologically shown to correspond to retinal deposits anterior to the retinal pigment epithelium (RPE) in contrast to the subretinal pigment epithelial location of soft drusen.<sup>5-7</sup> Distinctive clinical characteristics of RPD are the typical incomplete or complete ring-shaped pattern with initial spar-

ing of the fovea in contrast to soft drusen, which are typically located in central retinal areas, as well as the higher associated risk of progression to late stages including atrophy development.<sup>8-12</sup> Moreover, a higher incidence of RPD and development of multifocal lesions of macular neovascularization type 3 (MNV 3) has been recently described, which were typically more likely distributed in the temporal perifoveal area corresponding to the predominant pattern of RPD distribution.<sup>13,14</sup> In this context Sadda and coworkers<sup>12</sup> demonstrated in a meta-analysis that atrophy development often occurred in context of MNV treated with anti-vascular endothelial growth factor (VEGF) therapy; however,

at the same time it remained unclear whether anti-VEGF treatment is a causal reason for atrophy or rather associated with atrophy development. Besides RPD counting as a high-risk factor for retinal atrophy and corresponding progressive visual impairment, a putative association of RPD and systemic cardiovascular diseases has been suggested in previous studies.<sup>15,16</sup>

With the development of high-resolution retinal imaging in retinal diseases, microstructural changes of retinal layers have been detected in presence of RPD.<sup>9,17</sup> In this context, we previously reported on a localized reduction of the outer retina,<sup>18</sup> and Querques et al.<sup>19</sup> revealed an overall thinning of the choroid. Moreover, regression of subretinal deposits was shown to be associated with the development outer retinal atrophy, as well as a reduction of the underlying choroidal thickness.<sup>20,21</sup> Further optical coherence tomography angiography (OCT-A) studies reported a reduced choriocapillaris vessel density and a loss of choriocapillaris flow signal in RPD eyes in contrast to healthy control groups.<sup>22,23</sup>

Various studies found a functional impairment beyond best-corrected central visual acuity, using electroretinography (ERG) testing and fundus-controlled perimetry (FCP) (also termed as microperimetry).<sup>24–32</sup> A reduction of multifocal electroretinography (mfERG) function was seen in areas of RPD by Alten and coworkers.<sup>23</sup> In addition increased rod-intercept time (RIT) in presence of RPD was observed by Flamendorf et al.<sup>33</sup> whereas within a longitudinal observational period of 12 months RIT was shown to remain stable in eyes with AMD and RPD.<sup>34</sup> In another 12 months' follow-up study, a significant increase of RIT in eyes with RPD and iAMD was demonstrated in 14% of all testing points.<sup>35</sup> Interestingly there are further studies indicating a higher impairment of rod function within changing retinal eccentricity in eyes with RPD.<sup>26,34,36,37</sup> In this context highest impairment of rod function was found at 4° and 6° eccentricity of the fovea by Tan and coworkers,<sup>34</sup> whereas in another study highest abnormality of rod function in eyes with RPD was observed at 8° eccentricity after previous photobleach.<sup>26</sup>

FCP testing recently showed a localized reduction of mesopic and especially scotopic retinal sensitivity corresponding to areas with RPD secondary to AMD,<sup>25,27</sup> which could be previously linked to a localized thinning of the partial outer retinal layer thickness.<sup>18</sup> In another work Wu and coworkers<sup>38</sup> did not observe a significant association of functional changes in mesopic FCP testing within presence of RPD in a cross-sectional study, whereas a reduced multifocal electroretinography (mfERG) implicit time, as well as reduced function, was exhibited in areas of RPD.

In summary, recent findings underscore that eyes with predominantly RPD differ not only in terms of natural history and retinal function from eyes with soft drusen, but potentially also in terms of treatment response.<sup>27</sup> A subgroup analysis by Guymer et al.<sup>39</sup> suggests that eyes with RPD treated by subthreshold nanosecond laser have an increased risk for progression to late-stage disease compared to eyes with without RPD.

To date data on structural and functional changes in presence of RPD over time are limited. While the extension of areas with RPD, the increase of RPD density and the regression of individual lesions over time has been shown, the dynamics of progressive outer retinal degeneration associated with RPD lesions are yet poorly understood.<sup>18,20</sup> Further, it remains unclear how functional impairment is both temporally and spatially linked to RPD occurrence. This may be important for the design of clinical trials and the development of meaningful clinical endpoints in

AMD. In this context, the aim of the current study was to quantify thickness changes of different retinal layers over time and to both spatially and temporally evaluate the effects of morphological changes on mesopic and scotopic retinal sensitivity as assessed by FCP.

## METHODS

### Subjects

Subjects of the study were recruited at the Department of Ophthalmology at the University of Bonn, Bonn, Germany, and were monitored—in addition to the baseline visit—by three annual visits between June 2014 and February 2019 (total of four visits). For inclusion, eligibility criteria were the presence of RPD encompassing the size of at least two disc areas with at least one medium (>63 μm) or large (>125 μm) size druse in the context of AMD in either eye.<sup>2,25</sup> If both eyes of a patient met the inclusion criteria, both eyes were enclosed.

As controls, cross-sectional data of age-matched eyes without any signs of pathologic ocular changes (one eye of per subject) were included, i.e., no follow-up visits were performed in controls. For both subjects and controls, only eyes with clear media, visual acuity of a least logMAR 0.2, as well as stable fixation to enable functional testing and multimodal imaging, were included in this study.

Exclusion criteria included any signs of geographic atrophy (GA), MNV, diabetic retinopathy, glaucoma, prior laser treatments or prior intraocular surgery except for cataract surgery. AMD subjects and controls with refractive errors greater ±3 diopters spherical equivalent were excluded.

All participants received a complete ophthalmological examination including best-corrected visual acuity assessment (BCVA), slit lamp examination and fundus biomicroscopy.

The study protocol complied with the Declaration of Helsinki and was approved by the local ethics committee (Ethik-Kommission, Medizinische Fakultät, Rheinische Friedrich-Wilhelms-Universität; Lfd. Nr.125/14). After explaining the study procedures and possible consequences of participation, written consent of participation was obtained from each participant.

### Retinal Imaging

For retinal imaging a standardized imaging protocol was performed in subjects and controls after pupil dilation with 1.0% tropicamide and 2.5% phenylephrine. Simultaneous confocal scanning laser ophthalmoscopy (cSLO) and spectral-domain optical coherence tomography (SD-OCT) imaging was performed using the Spectralis HRA+OCT (Heidelberg Engineering, Heidelberg, Germany) device. The imaging protocol included color fundus photography, fundus autofluorescence (exc λ = 488 nm, em λ = 500–800 nm, minimum 15 frames), as well as combined cSLO near-infrared reflectance and SD-OCT imaging (high-speed mode, 30° × 25°, ART minimum 9 frames, 61 B-scan, distance 120 μm).

### Analysis of Retinal Thickness

For thickness analysis of retinal layers, volumetric SD-OCT data were initially automatically segmented with the Heidelberg Eye Explorer software (Spectralis Viewing Module 6.3.2.0; Heidelberg Engineering, Heidelberg, Germany).

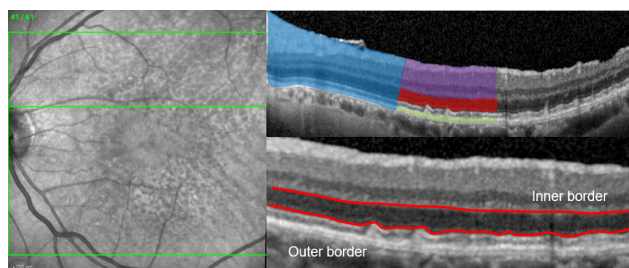


**FIGURE 1.** Spectral-domain optical coherence tomography raster scan (*left*) with the segmented retinal layers (*top right*) of the total retina (*blue*), the inner retina (*violet*), the pORL (*red*), and the RPEDC (*green*), as well as the boundaries (*bottom right—red colored*) for the assessment of the pORL thickness.

Each segmentation of the 61 B-scans was reviewed carefully and corrected manually if indicated. In our study we defined the total retinal thickness as the distance between the internal limiting membrane (ILM) and the Bruch's membrane (BM). The retinal-pigment-epithelium-drusen-complex (RPEDC) thickness was measured from the BM to the retinal-pigment-epithelium layer (RPE) including RPD. As previously reported,<sup>18</sup> the hyporeflective zone between the hyperreflective border of the outer plexiform layer (OPL; inner border) and the hyperreflective inner border of the ellipsoid zone (outer border) was defined as the partial outer retinal layer (pORL), (see Fig. 1). Due to the challenging discrimination of the ellipsoid zone (EZ) within presence of RPD, retinal thickness of the EZ was not included in this analysis. The inner retina was defined as the distance between the ILM and the OPL.

### Fundus-Controlled Perimetry

FCP was performed under scotopic and mesopic conditions in patients using the Nidek MP-1S device (Nidek Technologies, Padova, Italy). For each examination a test grid ( $10^\circ \times 10^\circ$ ) of 56-stimuli points was used, centered on the fovea of each eye. At each visit subjects started with the scotopic examination with dark adaptation of 20 minutes before testing. To handle the limited dynamic range for scotopic testing with the Nidek MP-1S device, each scotopic examination (Goldmann V, 200 ms, 4-2 strategy, background luminance  $0.0032 \text{ cd/m}^2$ ,  $3^\circ$  radius, and 1-pixel fixation ring) started with a filter selection test to determine the appropriate neutral density (ND) filter (0.0 log units, 1.0 log units and 2.0 log units). The pretest was used based on previous protocols following discussion with the manufacturer of the device.<sup>18,25</sup> Then, after a short break (less than five minutes) and ending dark adaptation, patients underwent mesopic testing (Goldmann III, 200 ms, 4-2 strategy, background luminance  $1.27 \text{ cd/m}^2$ ).

Because of the difficulties of a direct comparison of scotopic sensitivities within the different filter groups, results of functional testing in each study eye were only included in the current analysis, if there had been no change of the ND filter between baseline and the follow-up examinations. For the longitudinal analysis of retinal function, point-wise change of retinal sensitivity from baseline to the single follow-up visits was evaluated. Moreover retinal sensitivities in the different groups of retinal areas were compared to each other. With the use of combined confocal SLO infrared reflectance and spectral-domain (SD)-OCT, as well as fundus autofluorescence imaging, the following retinal areas were detected and compared with each other:

(a) areas with RPD being already present at baseline visit, (b) areas showing unremarkable pathological changes at any visit, and finally (c) areas with new RPD lesions developing during follow-up visits.

### Pointwise Correlation of Retinal Sensitivity to Localized Retinal Layer Thickness

As previously reported in a recent work by Pfau and coworkers,<sup>27</sup> for the analysis of retinal layer thickness at the corresponding stimulus location of FCP testing, volumetric thickness maps for each layer were transferred as tab-delimited file to Image J (U.S. National Institutes of Health, Bethesda, MD, USA). The FCP data were registered and aligned to the outer retina to the SD-OCT en face image in Image J using nonlinear affine transformation according to retinal vessel bifurcations. Then, the position of each FCP stimulus location as marked on the SD-OCT en face image with the tracing tool provided by Image J. Finally, retinal thickness at the site of each stimulus location and area for scotopic (Goldmann V 1.7°) test stimuli were extracted from the SD-OCT for each layer using the measure function in Image J.

### Statistical Analysis

Statistical analyses were performed using the software program R. Snellen fractions of visual acuity measurement were converted to the LogMAR chart. At baseline mean retinal sensitivities and mean retinal thickness values were analyzed in areas of RPD and unremarkable regions of the retina. For retinal thickness analysis, thickness values were normalized (z-scores) based on the corresponding normative mean value and normative standard deviation (SD) derived from the age-matched control group. For the longitudinal analysis, baseline differences of retinal thickness and retinal sensitivity values were evaluated. To account for derived variations in retinal layer thickness caused by horizontal and vertical directions, spatial coordinates of each test stimuli and eye were taken into consideration to correct for the topographic variations between eyes. Then mixed-linear effect models were applied for the structure-function analysis.

## RESULTS

### Demographics

Thirty eyes of 25 AMD patients (mean age 72.1 years, interquartile range [IQR; 70.19–79.80], range 62.0–86.9; 16 females, 10 pseudophakic eyes) and 19 eyes of 19 controls (mean age 71.5 years, IQR [69.7–76.5], range 67–89; 11 females, 1 pseudophakic eye) were included at baseline. FCP testing was performed in 18 eyes using the ND 1.0 filter, in 12 eyes the ND 2.0 filter was applied. Follow-up examinations were performed at month 12 (FU1) in 20 eyes, at month 24 (FU2) in 12 and at month 36 (FU3) in 11 eyes, respectively. Eyes were excluded from follow-up examinations in case of a conversion to macular neovascularization ( $n = 1$  at FU2) or in case of a ND filter change ( $n = 6$  at FU1;  $n = 3$  at FU2;  $n = 1$  at FU3). Further follow-up data of eight eyes were not available because subjects were no longer willing or able (because of general illness) to further participate in the study ( $n = 4$  at FU1;  $n = 4$  at FU2; and  $n = 0$  at FU3). Table 1 gives an overview on patient data available at each time of follow-up visit and detailed reasons

**TABLE 1.** Overview of the Number of Follow-Up Visits and Reasons For Study Exits in the Patient Cohort

Patient Study Cohort	Baseline	FU1	FU2	FU3
Number of assessed patients' eyes for analysis				
Total	30	20	12	11
Number of study exits				
Exit b/o conversion into macular neovascularization (MNV)	/	0	1	0
Exit b/o ND filter change	/	6	3	1
Exit b/o general illness	/	4	4	0

b/o, because of.

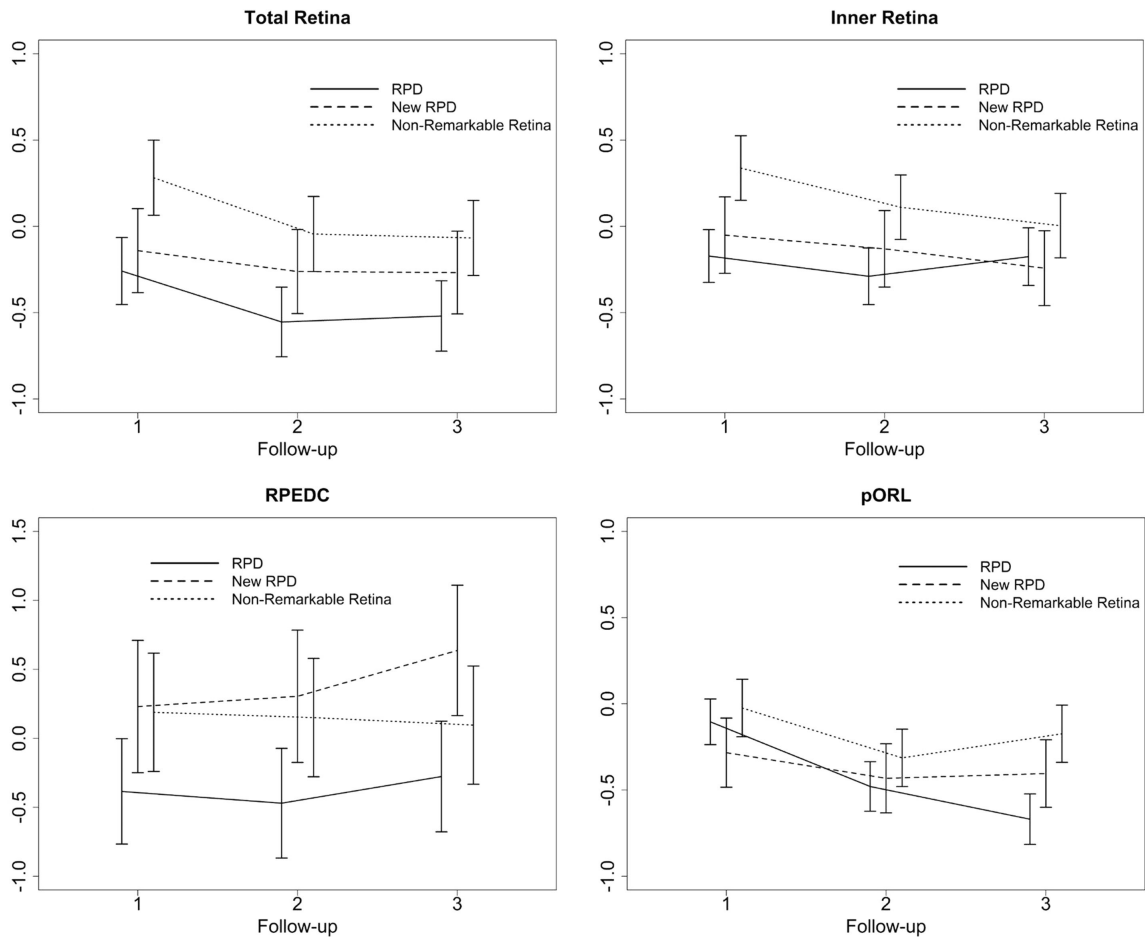


**FIGURE 2.** Graphical illustration of the longitudinal thickness changes in SD of the control group of the total retina, the inner retina, the RPEDC, and the pORL thickness. For each of the four layers, the changes are shown for the three different groups: (a) regions of existing RPD at baseline, (b) regions of newly developing RPD, and (c) in non-remarkable regions of the retina. Data of the retinal thickness change were plotted in normative SD. The x-axis shows the number of the follow-up visit.

for study exits. Eyes that were once excluded at follow-up visit did not receive a follow-up examination at a later time point.

Mean BCVA at baseline was logMAR 0.1 (Snellen equivalent 20/25; IQR [0.0–0.2] range 0.3–0.0). Over three years, a slight decline in BCVA was observable with a mean of logMAR 0.1 (Snellen equivalent 20/25; IQR [0.1–0.2] range 0.4–0.0) at FU1, of logMAR 0.2 (Snellen equivalent 20/32; IQR [0.0–0.3] range 0.0–0.5) at FU2 and of logMAR 0.2 (Snellen equivalent 20/32; IQR [0.1–0.4] range 0.0–0.4) at FU3.

**Cross-Sectional Retinal Thickness Analysis**

At baseline, retinal thickness of the pORL was reduced in areas with RPD with a thickness (mean ± SD) of  $70.21 \pm 7.09 \mu\text{m}$  compared to  $77.47 \pm 5.02 \mu\text{m}$  in unremarkable retinal regions (difference  $-7.26 [-6.32; -8.20]$ , 95% confidence interval [CI],  $P < 0.001$ ). At baseline the total retina, the RPEDC, and the inner retina were thicker in areas with RPD compared with areas with unremarkable pathological alterations. For more detailed results, also see Supplemental Tables S1 and S2.

## Longitudinal Change of Retinal Thickness

Comparing results of longitudinal retinal thickness changes, the pORL layer thickness exhibited a significant decrease over time. After three years, the pORL decreased by (estimate  $\pm$  standard error [SE])  $-0.668 \pm 0.07$  SD (SD of the control group) ( $P < 0.001$ ) in areas with RPD, followed by  $-0.404 \pm 0.10$  SD ( $P < 0.001$ ) in new occurring RPD regions and to a lesser extent by  $-0.173 \pm 0.08$  SD ( $P = 0.041$ ) in unremarkable regions. This corresponds in terms of thickness deviation (i.e., accounting for the spatial variation of normative mean thickness, but not for the spatial variation in normative thickness variability) to  $-12.5$   $\mu$ m in areas with RPD,  $-7.6$   $\mu$ m in areas with new RPD and to  $-3.2$   $\mu$ m in unremarkable regions (non-RPD). In addition, longitudinal retinal thickness analysis revealed higher retinal layer thicknesses changes in any areas affected by RPD compared with unremarkable areas of the retina. Interestingly, longitudinal retinal thickness changes in areas with new arising RPD were higher for the inner retina (i.e., retinal thinning) and the RPEDC (i.e., retinal thickening) compared with thickness changes in areas with previous existing RPD.

More detailed results of the longitudinal retinal layer thickness alterations with corresponding thickness deviations are illustrated in Figure 2 and Table 2. Moreover, a representative patient example of sensitivity and pORL thickness changes in areas of RPD over three years is shown in Figure 3.

## Cross-Sectional Functional Analysis

At baseline, a total of 1680 test stimuli measured in 30 eyes was available for analysis, of which 952 test points were in RPD areas and 670 in unremarkable areas. The mean sensitivity in RPD regions was (mean  $\pm$  SD)  $16.60 \pm 0.69$  dB; (95% CI 15.13; 18.0) in mesopic and  $12.14 \pm 0.65$  dB; (10.75; 15.53) in scotopic testing using the ND 1.0 filter. These values were markedly reduced as compared with unremarkable areas, showing mean sensitivities of  $18.72 \pm 0.35$  dB; (17.97; 19.47; mesopic) and  $18.67 \pm 0.33$  dB (17.96; 19.37; scotopic). Similar observations were made in eyes that required the ND 2.0 filter (RPD area sensitivity:  $18.14 \pm 0.66$  dB; [16.68; 19.59] for mesopic and  $16.35 \pm 0.31$  dB; [15.67; 17.05] for scotopic testing; unremarkable area sensitivity  $19.07 \pm 0.36$  dB; [18.26; 19.88] for the mesopic and  $18.10 \pm 0.51$  dB; [16.97; 19.23] for the scotopic examination).

## Change of Retinal Sensitivity Over Time

Taking a look at longitudinal retinal sensitivity changes resulting from a regression model, mesopic function showed a change of (estimate  $\pm$  SE)  $-7.76 \pm 0.51$  dB ( $P < 0.0001$ ) in RPD regions and of  $-3.12 \pm 0.59$  dB ( $P < 0.0001$ ) in unremarkable regions after three years. Scotopic retinal function exhibited a change of  $-3.51 \pm 0.74$  dB ( $P < 0.0001$ ) for RPD and of  $0.32 \pm 0.77$  dB ( $P = 0.6799$ ) for unremarkable regions during these three years.

In region that developed "de novo" RPD, a reduction in both mesopic and scotopic retinal sensitivity was observed with a mean decrease in mesopic sensitivity of  $-1.89 \pm 0.72$  dB ( $P = 0.0096$ ) at FU1,  $-4.76 \pm 0.72$  dB ( $P < 0.0001$ ) at FU2 and  $-5.97 \pm 0.70$  dB ( $P < 0.0001$ ) at FU3 and changes of scotopic sensitivity of  $-0.48 \pm 0.83$  dB ( $P = 0.569$ ) at FU1,  $-2.55 \pm 0.83$  dB ( $P = 0.0039$ ) at FU2 and  $-2.06 \pm 0.82$

dB ( $P = 0.0168$ ) at FU3. Detailed results of the longitudinal sensitivity changes are shown in Figure 4 and Table 3.

## Topographic Comparison of Longitudinal Retinal Thickness and Sensitivity Changes

Comparing the topographic variation of longitudinal retinal thickness changes for each retinal layer and each area (with or without RPD), detailed analysis revealed significant higher losses of pORL thickness in areas of RPD and new RPD within the central  $2^\circ$  to  $6^\circ$  of the retina compared to thickness changes within the more peripheral retina ( $8^\circ$ – $10^\circ$ ). No significant longitudinal thickness changes between the center and the periphery were noted for the total retina, the inner retina, and the RPEDC. Interestingly, total values of RPEDC layer thickness changes were higher in areas with new arising RPD within the central  $6^\circ$  of the retina compared with the periphery.

The retinal sensitivity changes over time of both mesopic and scotopic sensitivity did not differ between the central and peripheral retina. Nevertheless total values of retinal sensitivity changes were higher for mesopic and scotopic FCP testing in areas with RPD and New RPD in the central retina compared to sensitivity changes outside of the central  $6^\circ$ . Supplementary Tables S3A and S3B demonstrate the detailed boxplots on the longitudinal topographic distribution of the corrected retinal layer thickness changes, as well as mesopic and scotopic sensitivity changes.

## Structure Function Analysis

Mixed-effect models considering the effect of retinal thickness alone on retinal sensitivity disclosed no significant effect of retinal thickness of the total retina ( $-0.134 \pm 0.32$  dB per Z-score of FRT;  $P = 0.67$ ) and the inner retina ( $-0.35 \pm 0.25$  dB per Z-score of IRT;  $P = 0.174$ ) on scotopic retinal function. However, for the RPEDC and the pORL layer, both the retinal thickness, as well as the absence/presence of RPD demonstrated a significant effect on scotopic retinal function ( $-0.94 \pm 0.18$  dB per Z-score of RPEDC;  $P < 0.001$  and  $1.16 \pm 0.27$  dB per Z-score of pORL;  $P < 0.001$ ). A significant interaction effect between the pORL thickness and the absence of RPD was not observed at baseline visit ( $P = 0.155$ ). Moreover, pORL thickness change of 1 SD was correlated to a sensitivity reduction of 3.47 dB in scotopic and of 0.79 dB in mesopic FCP testing, respectively,  $P < 0.001$ . Although inner retinal thickness exhibited no significant association with scotopic function alone, test stimuli coinciding with unremarkable retina exhibited a significantly higher scotopic sensitivity ( $+3.87 \pm 0.17$  dB,  $P < 0.001$ ). With regard to structure-function correlations for mesopic retinal sensitivity, similar significant associations between retinal layer thicknesses and retinal function were observed, although general estimated mesopic retinal sensitivity was higher and less reduced in presence of RPD compared with scotopic testing (also see Supplemental Table S4).

## DISCUSSION

This longitudinal natural-history study demonstrates that eyes with intermediate AMD (iAMD) and predominantly RPD are characterized by both progressive outer retinal degeneration and functional decline. These structural and functional impairments are especially pronounced in regions

TABLE 2. Detailed Results of the Longitudinal Retinal Thickness Changes\*

Retinal Thickness	Area	Follow Up 1			Follow Up 2			Follow Up 3		
		Estimates (in SD)	SE (in SD)	P Value	Estimates (in SD)	SE (in SD)	P Value	Estimates (in SD)	SE (in SD)	P Value
Total Retina	RPD	-0.258	0.09	P = 0.011	-0.553	0.09	P < 0.001	-0.519	0.09	P < 0.001
	New RPD	-0.140	0.12	P = 0.254	-0.262	0.12	P = 0.036	-0.267	0.12	P = 0.029
	Non-RPD	0.282	0.11	P = 0.124	-0.044	0.11	P = 0.683	-0.067	0.11	P = 0.535
Inner Retina	RPD	-0.171	0.07	P = 0.029	-0.289	0.08	P = 0.001	-0.175	0.08	P = 0.040
	New RPD	-0.050	0.11	P = 0.653	-0.130	0.11	P = 0.248	-0.242	0.10	P = 0.029
	Non-RPD	0.337	0.09	P = 0.001	0.111	0.09	P = 0.239	0.004	0.09	P = 0.964
RPED-Complex	RPD	-0.384	0.18	P = 0.049	-0.470	0.19	P = 0.022	-0.276	0.19	P = 0.165
	New RPD	0.230	0.24	P = 0.339	0.304	0.24	P = 0.209	0.637	0.23	P = 0.009
	Non-RPD	0.188	0.21	P = 0.378	0.150	0.21	P = 0.483	0.096	0.21	P = 0.653
pORL	RPD	-0.104	0.06	P = 0.118	-0.479	0.07	P < 0.001	-0.668	0.07	P < 0.001
	New RPD	-0.282	0.10	P = 0.005	-0.431	0.10	P < 0.001	-0.404	0.09	P < 0.001
	Non-RPD	-0.024	0.08	P = 0.773	-0.313	0.08	P < 0.001	-0.173	0.08	P = 0.041

\* The z-scores (estimate ± SE) in SD of the control group at each follow-up visit (FU 1, FU 2, FU 3) in regions with RPD, new arising regions of RPD (New RPD), and unremarkable regions of RPD (Non-RPD) with the corresponding longitudinal P values (FU visit to baseline visit). For comparison we provided the estimates in terms of thickness deviation from the spatially corresponding normative value. However, compared to z-scores, these do not take into account for the normative variability in thickness varies across the retina.

Estimates as Thickness Deviation (in μm)

Estimates (in SD)

Estimates as Thickness Deviation (in μm)

Estimates (in SD)

Estimates as Thickness Deviation (in μm)

Estimates (in SD)

Estimates as Thickness Deviation (in μm)

Estimates (in SD)

TABLE 3. Longitudinal Sensitivity Changes\*

FCP Examination	Region	FU1	FU2	FU3
Mesopic	RPD	-3.68 ± 0.46 dB ( <i>P</i> < 0.0001)	-7.19 ± 0.50 dB ( <i>P</i> < 0.0001)	-7.76 ± 0.51 dB ( <i>P</i> < 0.0001)
	New RPD	-1.89 ± 0.72 dB ( <i>P</i> = 0.0096)	-4.76 ± 0.72 dB ( <i>P</i> < 0.0001)	-5.97 ± 0.70 dB ( <i>P</i> < 0.0001)
	Non-RPD	-2.63 ± 0.59 dB ( <i>P</i> < 0.0001)	-4.63 ± 0.59 dB ( <i>P</i> = 0.0004)	-3.12 ± 0.59 dB ( <i>P</i> < 0.0001)
Scotopic	RPD	-1.18 ± 0.72 dB ( <i>P</i> = 0.1166)	-3.50 ± 0.73 dB ( <i>P</i> < 0.0001)	-3.51 ± 0.74 dB ( <i>P</i> < 0.0001)
	New RPD	-0.48 ± 0.83 dB ( <i>P</i> = 0.569)	-2.55 ± 0.83 dB ( <i>P</i> = 0.0039)	-2.06 ± 0.82 dB ( <i>P</i> = 0.0168)
	Non-RPD	-0.23 ± 0.77 dB ( <i>P</i> = 0.7612)	-0.57 ± 0.77 dB ( <i>P</i> = 0.4654)	0.32 ± 0.77 dB ( <i>P</i> = 0.6800)

\* Estimate ± standard error deriving from a regression model at each follow-up (FU) visit of mesopic and scotopic FCP testing in regions with RPD, new arising regions of RPD (New RPD), and unremarkable regions of RPD (Non-RPD) corresponding to Figure 4 with longitudinal *P* values (follow-up visit to baseline visit).

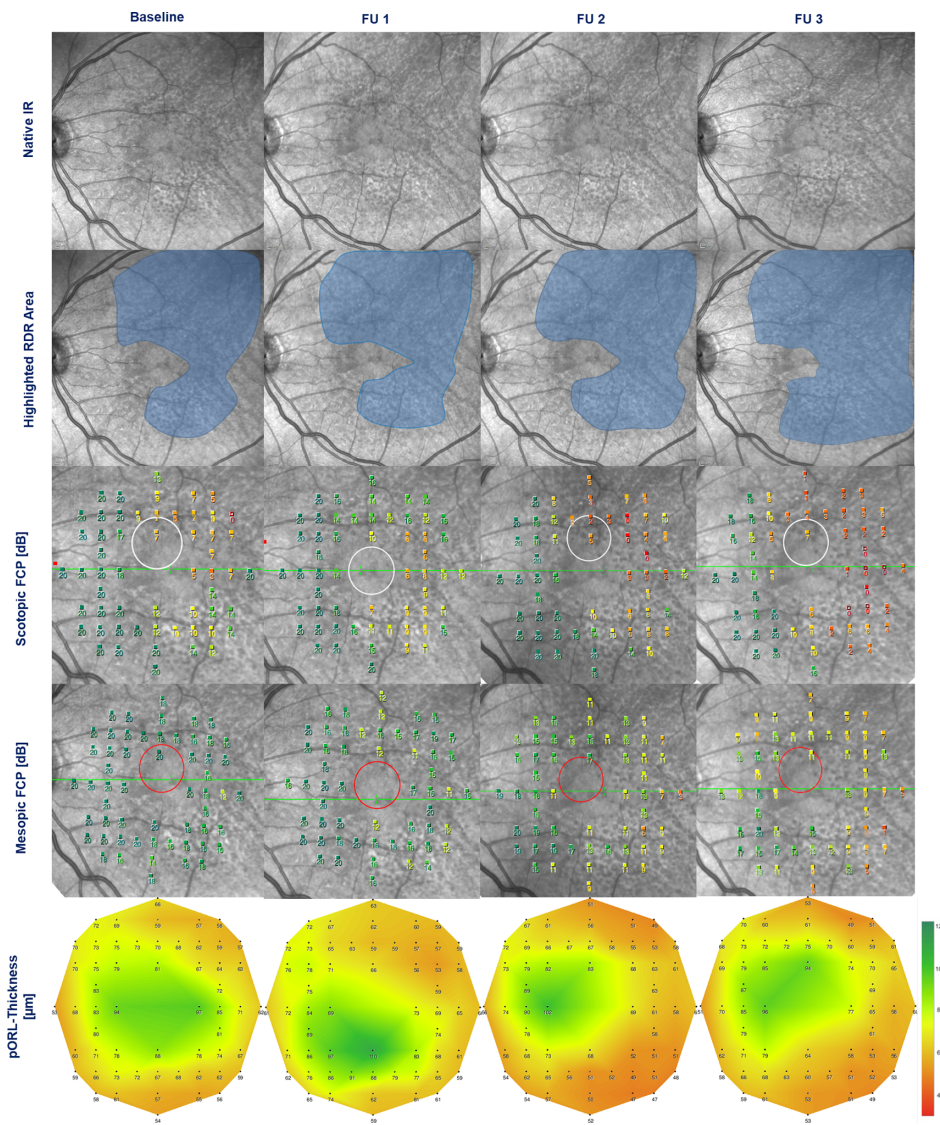
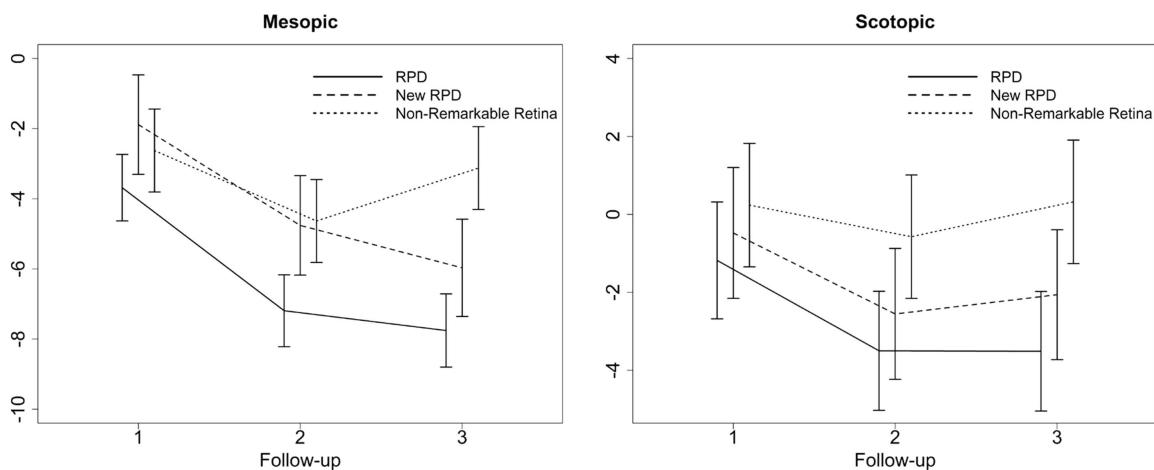


FIGURE 3. Representative example of a 72-year-old AMD patient with RPD in his left eye. Structural and functional data are illustrated for each visit (from left to right: baseline, follow-up 1 [FU 1], follow-up 2 [FU 2], and follow-up 3 [FU 3]). Extension area of RPD is shown by near-infrared cSLO imaging (first row: native images, second row: area involved highlighted by blue color). Corresponding functional testing is shown for mesopic (third row) and scotopic (fourth row) FCP. Thickness of the pORL (fifth row) is illustrated by a “heat map.” Note the increase in area extension of RPD over time, spatially and temporally corresponding to progressive thinning of the pORL and increasing loss of mesopic and scotopic retinal sensitivity.



**FIGURE 4.** Graphical illustration of the longitudinal sensitivity changes [estimate  $\pm$  standard error] in dB for mesopic and scotopic FCP testing at each follow-up visit (FU 1–3). Results are presented for retinal regions with RPD, newly developing RPD at follow-up visit, and regions with nonremarkable pathological alterations.

with RPD at baseline and newly developing RPD during the review period. Moreover, this study shows a point-wise correlation of pORL thinning to a localized loss of mesopic and scotopic retinal sensitivity.

Of all retinal layers tested and compared to controls, the pORL layer exhibited the most pronounced reduction of thickness in RPD regions (both existing and new occurring) at baseline and longitudinally. These observations that were made by comparing different regions within eyes would be in line to the findings reported by Ramon et al. of a faster thinning of ONL layer thickness in eyes with RPD within two years as compared to eyes with soft drusen.<sup>40</sup> In addition, results of a progressive pORL thinning do not only characterize outer retinal degeneration, but also point at underlying dynamic retinal processes of drusen as for example in this context RPD regression within a longitudinal period. For the RPEDC for example, a significant retinal layer thickening was exhibited in areas with New RPD, while progressive RPEDC thinning was shown within the longitudinal period in areas of previous existing RPD. Of note, Y. Zhang and coworkers were recently able to precisely describe the trajectories of progression and regression of individual RPD using adaptive optics scanning laser ophthalmoscopy (AOSLO).<sup>21</sup> By extension, we could now demonstrate that this lifecycle of RPD is indeed associated with a functional loss in terms of mesopic and scotopic retinal sensitivity.<sup>7</sup> It would be well conceivable that these observations would reflect progressive loss of photoreceptor integrity. Comparing longitudinal retinal thickness changes between the different retinal layers, findings moreover exhibited a trend towards a thinning of the inner retina in areas of RPD. Although previous cross-sectional studies could not find thickness changes of the inner retina in areas above drusen,<sup>41,42</sup> results of the structure-function analysis of this study indicated a significant association of the inner retinal layer thickness in presence of RPD with mesopic and scotopic retinal function. This observation may be explained by secondary changes to the inner retinal layers after the pronounced thinning of the pORL in association with RPD. Further longitudinal studies with longer follow-up time and also including follow-up data of healthy controls are here needed to further analyze the impact of the inner retina on retinal function.

In addition, findings of higher retinal layer thicknesses and retinal sensitivity changes within the central  $2^\circ$  to  $6^\circ$  retina compared with the periphery ( $8^\circ$ – $10^\circ$ ) correspond to the predominant perifoveal distribution of RPD, as well as to previous findings on rod mediated retinal function by Flynn and coworkers.<sup>36</sup>

Compared with previous cross-sectional structural-functional studies,<sup>26,33,43</sup> using dark-adapted microperimetry, rod-mediated dark adaptation and also electroretinography, this study confirms the strong spatial correlation between the thinning of the outer retina and impairment of both rod and cone function that was present at all four visits tests during the longitudinal observation.

RPD represent subtle lesions and their detection requires high-resolution imaging that was accomplished by multimodal imaging. Our findings demonstrate that dynamic changes in structure can be reliably quantified over an observation time of three years using current imaging technology. Future technological developments might improve detection of microstructural changes in more detail, potentially allowing to assess dynamic changes in shorter follow-up times.

At baseline we demonstrated a more pronounced loss of scotopic than mesopic sensitivity, whereas structural correlation was stronger for scotopic than mesopic FCP testing. Over time progressive reduction of sensitivity loss was larger for mesopic as compared with scotopic testing. This observation might indicate earlier deterioration of rod photoreceptors with subsequent cone degeneration during the life cycle of RPD corresponding to previous histopathologic findings on photoreceptor degeneration in context of AMD.<sup>44,45</sup> However, the limited dynamic range of the system, resulting in floor and ceiling effects, might also contribute to this observation.<sup>46</sup> After the initiation of this study, FCP devices with greater dynamic ranges have become available in the meantime.<sup>27,46</sup> The use of these new devices would be helpful to further investigate different degrees of progressive rod and cone dysfunction over time in the presence of RPD.

Previously, Wu et al.<sup>47</sup> reported on an estimated localized loss of mesopic sensitivity of  $-0.29$  dB per  $10\text{-}\mu\text{m}$  RPEDC thickening in eyes with large drusen and with or without RPD in iAMD. This study, including scotopic sensitivity assessment, also demonstrated pointwise structural-functional correlations along with RPEDC thick-

ening. Hereby, the range of sensitivity loss of  $-0.34$  dB for mesopic and  $-0.94$  dB for scotopic function per 1 SD RPEDC thickening would be comparable to the work by Wu et al.<sup>47</sup> In addition to challenges with FCP testing as outlined above, the sample size of this study was limited, and follow-up data were not available for all subjects. Although this study demonstrates a clear association of structure and function and its progression over time, detection of RPD and associated morphologic, as well as fine-detailed, functional changes can be subtle. A larger sample size with extensive follow-up would potentially allow to further investigate the extent and dynamics of structural and functional changes in the presence of RPD in more detail. For now, this study provides—to the best of our knowledge—for the first time detailed testing results at well-defined follow-up time points over three years, allowing us to estimate the progression of structural and functional change in the presence of RPD. The results of this study will be helpful to design and conduct future study on the structural and functional impairment in AMD patients.

In summary, this study provides data on the progression of structural and functional changes in the presence of RPD. It confirms previous cross-sectional reports of a localized correlation of pORL thinning and more severe rod than cone functional impairment, demonstrating that these observations are consistently present at each time point over three years. Moreover, the progressive nature of these degenerative changes can be accurately quantified. Structural and functional changes in newly occurring RPD areas also underscore the pathological relevance of RPD lesions in course of AMD disease. The results of the study suggest that thinning of the pORL and assessment of both scotopic and mesopic FCP may represent attractive structural and functional biomarkers for future interventional clinical trials in AMD.

### Acknowledgments

The authors thank Verena Bonn for the administrative support in data acquisition and analysis.

Supported by research grants of the Rudolf and Anna Katharina Eichenauer-Foundation, the German Research Foundation (Deutsche Forschungsgemeinschaft PF 950/1-1) and in part by an Unrestricted Grant from Research to Prevent Blindness, New York, NY, to the Department of Ophthalmology & Visual Sciences, University of Utah.

Disclosure: **M. Sassmannshausen**, Heidelberg Engineering (F); Carl Zeiss Meditec (F); Optos (F); CenterVue (F); **M. Pfau**, Heidelberg Engineering (F); Carl Zeiss Meditec (C, F); Optos (F); CenterVue (F); **S. Thiele**, Heidelberg Engineering (F, R); Carl Zeiss Meditec (F); Optos (F); CenterVue (F); Bayer (R); Novartis (R); **R. Fimmers**, None; **J. Steinberg**, None; **M. Fleckenstein**, Heidelberg Engineering (F); Novartis (C, F); Roche/Genentech (C); US20140303013A1 (P); **F. Holz**, Acucela (C, F, R); Allergan (F, R); Appelis (C, R); Bayer (C, F, R); Boehringer-Ingelheim (C); Bioeq/Formycon (F, C); CenterVue (F); Ellex (R); Roche/Genentech (C, F, R); Geuder (C); Grayburg Vision (C, R); Heidelberg Engineering (C, F, R); Kanghong (C, F); LinBioscience (C, R); NightStarX (F); Novartis (C, F, R); Optos (F); Pixium Vision (C, F, R); Oxurion (C, R); Stealth BioTherapeutics (C, R); Carl Zeiss Meditec (F, R); **S. Schmitz-Valckenberg**, Acucela (F); Alcon/Novartis (C, F, R); Allergan (C, F, R); Bayer (F, R); Bioeq/Formycon (F, C); Carl Zeiss Meditec (F, R); CenterVue (F); Galimedix (C); Genentech/Roche (F, R); Heidelberg Engineering (F); Katairo (F); Optos (F)

### References

1. Lim LS, Mitchell P, Seddon JM, Holz FG, Wong TY. Age-related macular degeneration. *The Lancet*. 2012;379:1728–1738.
2. Ferris FL, Wilkinson CP, Bird A, et al. Clinical classification of age-related macular degeneration. *Ophthalmology*. 2013;120:844–851.
3. Schmitz-Valckenberg S, Steinberg JS, Fleckenstein M, Visvalingam S, Brinkmann CK, Holz FG. Combined confocal scanning laser ophthalmoscopy and spectral-domain optical coherence tomography imaging of reticular drusen associated with age-related macular degeneration. *Ophthalmology*. 2010;117:1169–1176.
4. Zweifel SA, Spaide RF, Curcio CA, Malek G, Imamura Y. Reticular pseudodrusen are subretinal drusenoid deposits. *Ophthalmology*. 2010;117:303–312.e1.
5. Curcio CA, Messinger JD, Sloan KR, McGwin G, Medeiros NE, Spaide RF. Subretinal drusenoid deposits in non-neovascular age-related macular degeneration: morphology, prevalence, topography, and biogenesis model. *Retina*. 2013;33:265–276.
6. Greferath U, Guymer RH, Vessey KA, Brassington K, Fletcher EL. Correlation of Histologic Features with In Vivo Imaging of Reticular Pseudodrusen. *Ophthalmology*. 2016;123:1320–1331.
7. Chen L, Messinger JD, Zhang Y, Spaide RF, Freund KB, Curcio CA. Subretinal drusenoid deposit in age-related macular degeneration: histologic insights into initiation, progression to atrophy, and imaging. *Retina*. 2020;40:618–631.
8. Steinberg JS, Fleckenstein M, Holz FG, Schmitz-Valckenberg S. Foveal sparing of reticular drusen in eyes with early and intermediate age-related macular degeneration. *Invest Ophthalmol Vis Sci*. 2015;56:4267–4274.
9. Schmitz-Valckenberg S, Alten F, Steinberg JS, et al. Reticular drusen associated with geographic atrophy in age-related macular degeneration. *Invest Ophthalmol Vis Sci*. 2011;52:5009–5015.
10. Steinberg JS, Göbel AP, Fleckenstein M, Holz FG, Schmitz-Valckenberg S. Reticular drusen in eyes with high-risk characteristics for progression to late-stage age-related macular degeneration. *Br J Ophthalmol*. 2015;99:1289–1294.
11. Auge J, Steinberg JS, Fleckenstein M, Holz FG, Schmitz-Valckenberg S. Reticular drusen over time with SD-OCT. *Der Ophthalmologe*. 2014;111:765–771.
12. Sadda SR, Guymer R, Monés JM, Tufail A, Jaffe GJ. Anti-vascular endothelial growth factor use and atrophy in neovascular age-related macular degeneration: systematic literature review and expert opinion. *Ophthalmology*. 2020;127:648–659.
13. Haj Najeeb B, Deak G, Schmidt-Erfurth U, Gerendas BS. The RAP Study, report two: the regional distribution of macular neovascularization type 3, a novel insight into its etiology. *Retina*. 2020;ePub ahead of print.
14. Kim JH, Chang YS, Kim JW, Kim CG, Lee DW. Characteristics of type 3 neovascularization lesions: focus on the incidence of multifocal lesions and the distribution of lesion location. *Retina*. 2020;40:1124–1131.
15. Fleckenstein M, Schmitz-Valckenberg S, Lindner M, et al. The "diffuse-trickling" fundus autofluorescence phenotype in geographic atrophy. *Invest Ophthalmol Vis Sci*. 2014;55:2911–2920.
16. McGuinness MB, Finger RP, Karahalios A, et al. Age-related macular degeneration and mortality: the Melbourne Collaborative Cohort Study. *Eye (London, England)*. 2017;31:1345–1357.
17. Khanifar AA, Koreishi AF, Izatt JA, Toth CA. Drusen ultrastructure imaging with spectral domain optical coherence

- tomography in age-related macular degeneration. *Ophthalmology*. 2008;115:1883–1890.
18. Steinberg JS, Sassmannshausen M, Fleckenstein M, et al. Correlation of Partial Outer Retinal Thickness With Scotopic and Mesopic Fundus-Controlled Perimetry in Patients With Reticular Drusen. *Am J Ophthalmol*. 2016;168:52–61.
  19. Querques G, Querques L, Forte R, Massamba N, Coscas F, Souied EH. Choroidal changes associated with reticular pseudodrusen. *Invest Ophthalmol Vis Sci*. 2012;53:1258–1263.
  20. Spaide RF. Outer retinal atrophy after regression of RDR. *Retina*. 2013;33:1800–1808.
  21. Zhang Yuhua. Lifecycles of individual subretinal drusenoid deposits and evolution of outer retinal atrophy in age-related macular degeneration. *Ophthalmol Retina*. 2020;4:274–283. 2019.
  22. Nesper PL, Soetikno BT, Fawzi AA. Choriocapillaris nonperfusion is associated with poor visual acuity in eyes with reticular pseudodrusen. *Am J Ophthalmol*. 2017;174:42–55.
  23. Alten F, Heiduschka P, Clemens CR, Eter N. Longitudinal structure/function analysis in reticular pseudodrusen. *Invest Ophthalmol. Vis. Sci*. 2014;55:6073.
  24. Cocce KJ, Stinnett SS, Luhmann UFO, et al. Visual function metrics in early and intermediate dry age-related macular degeneration for use as clinical trial endpoints. *Am J Ophthalmol*. 2018;189:127–138.
  25. Steinberg JS, Fitzke FW, Fimmers R, Fleckenstein M, Holz FG, Schmitz-Valckenberg S. Scotopic and photopic microperimetry in patients with reticular drusen and age-related macular degeneration. *JAMA Ophthalmol*. 2015;133:690–697.
  26. Tan R, Guymer RH, Luu CD. Subretinal drusenoid deposits and the loss of rod function in intermediate age-related macular degeneration. *Invest Ophthalmol Vis Sci*. 2018;59:4154–4161.
  27. Pfau M, Lindner M, Gliem M, et al. Mesopic and dark-adapted two-color fundus-controlled perimetry in patients with cuticular, reticular, and soft drusen. *Eye (London, England)*. 2018;32:1819–1830.
  28. Welker SG, Pfau M, Heinemann M, Schmitz-Valckenberg S, Holz FG, Finger RP. Retest reliability of mesopic and dark-adapted microperimetry in patients with intermediate age-related macular degeneration and age-matched controls. *Invest Ophthalmol Vis Sci*. 2018;59:AMD152–AMD159.
  29. Pondorfer SG, Terheyden JH, Heinemann M, Wintergerst MWM, Holz FG, Finger RP. Association of vision-related quality of life with visual function in age-related macular degeneration. *Sci Rep*. 2019;9:15326.
  30. Midena E, Vujosevic S, Convento E, Manfre' A, Cavarzeran F, Pilotto E. Microperimetry and fundus autofluorescence in patients with early age-related macular degeneration. *Br J Ophthalmol*. 2007;91:1499–1503.
  31. Midena E, Pilotto E. Microperimetry in age-related macular degeneration. *Eye (London, England)*. 2017;31:985–994.
  32. Ooto S, Ellabban AA, Ueda-Arakawa N, et al. Reduction of retinal sensitivity in eyes with reticular pseudodrusen. *Am J Ophthalmol*. 2013;156:1184–1191.e2.
  33. Flamendorf J, Agrón E, Wong WT, et al. Impairments in dark adaptation are associated with age-related macular degeneration severity and reticular pseudodrusen. *Ophthalmology*. 2015;122:2053–2062.
  34. Tan RS, Guymer RH, Aung K-Z, Caruso E, Luu CD. Longitudinal assessment of rod function in intermediate age-related macular degeneration with and without reticular pseudodrusen. *Invest Ophthalmol Vis Sci*. 2019;60:1511–1518.
  35. Nguyen CT, Fraser RG, Tan R, et al. Longitudinal changes in retinotopic rod function in intermediate age-related macular degeneration. *Invest Ophthalmol. Vis. Sci*. 2018;59:AMD19–AMD24.
  36. Flynn OJ, Cukras CA, Jeffrey BG. Characterization of rod function phenotypes across a range of age-related macular degeneration severities and subretinal drusenoid deposits. *Investigative ophthalmology & visual science*. 2018;59:2411–2421.
  37. Csaky KG, Patel PJ, Sepah YJ, et al. Microperimetry for geographic atrophy secondary to age-related macular degeneration. *Surv Ophthalmol*. 2019;64:353–364.
  38. Wu Z, Ayton LN, Makeyeva G, Guymer RH, Luu CD. Impact of reticular pseudodrusen on microperimetry and multifocal electroretinography in intermediate age-related macular degeneration. *Invest Ophthalmol Vis Sci*. 2015;56:2100–2106.
  39. Guymer RH, Wu Z, Hodgson LAB, et al. Subthreshold nanosecond laser intervention in age-related macular degeneration: the LEAD Randomized Controlled Clinical Trial. *Ophthalmology*. 2019;126:829–838.
  40. Ramon C, Cardona G, Biarnés M, Ferraro LL, Monés J. Longitudinal changes in outer nuclear layer thickness in soft drusen and reticular pseudodrusen. *Clinical & experimental optometry*. 2019;102:601–610.
  41. Schuman SG, Koreishi AF, Farsiu S, S-h Jung, Izatt JA, Toth CA. Photoreceptor layer thinning over drusen in eyes with age-related macular degeneration imaged in vivo with spectral-domain optical coherence tomography. *Ophthalmology*. 2009;116:488–496.e2.
  42. Sadigh S, Cideciyan AV, Sumaroka A, et al. Abnormal thickening as well as thinning of the photoreceptor layer in intermediate age-related macular degeneration. *Invest Ophthalmol. Vis. Sci*. 2013;54:1603–1612.
  43. Alten F, Heiduschka P, Clemens CR, Eter N. Multifocal electroretinography in eyes with reticular pseudodrusen. *Invest Ophthalmol Vis Sci*. 2012;53:6263–6270.
  44. Curcio CA, Owsley C, Jackson GR. Spare the rods, save the cones in aging and age-related maculopathy. *Invest Ophthalmol. Vis. Sci*. 2000;41:2015–2018.
  45. Curcio CA, Medeiros NE, Millican CL. Photoreceptor loss in age-related macular degeneration. *Invest Ophthalmol. Vis. Sci*. 1996;37:1236–1249.
  46. Steinberg JS, Sassmannshausen M, Pfau M, et al. Evaluation of two systems for fundus-controlled scotopic and mesopic perimetry in eye with age-related macular degeneration. *Transl Vis Sci Technol*. 2017;6:7.
  47. Wu Z, Cunefare D, Chiu E, et al. Longitudinal associations between microstructural changes and microperimetry in the early stages of age-related macular degeneration. *Invest Ophthalmol Vis Sci*. 2016;57:3714–3722.